NASA/TM-2000-209014

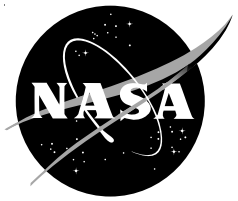

Design and Evaluation of a New Boundary-Layer Rake for Flight Testing

Trong T. Bui and David L. Oates
NASA Dryden Flight Research Center
Edwards, California

Jose C. Gonsalez
Dynacs Engineering Co., Inc.
Brookpark, Ohio

January 2000

The NASA STI Program Office…in Profile

Since its founding, NASA has been dedicated to the advancement of aeronautics and space science. The NASA Scientific and Technical Information (STI) Program Office plays a key part in helping NASA maintain this important role.

The NASA STI Program Office is operated by Langley Research Center, the lead center for NASA's scientific and technical information. The NASA STI Program Office provides access to the NASA STI Database, the largest collection of aeronautical and space science STI in the world. The Program Office is also NASA's institutional mechanism for disseminating the results of its research and development activities. These results are published by NASA in the NASA STI Report Series, which includes the following report types:

- TECHNICAL PUBLICATION. Reports of completed research or a major significant phase of research that present the results of NASA programs and include extensive data or theoretical analysis. Includes compilations of significant scientific and technical data and information deemed to be of continuing reference value. NASA's counterpart of peer-reviewed formal professional papers but has less stringent limitations on manuscript length and extent of graphic presentations.

- TECHNICAL MEMORANDUM. Scientific and technical findings that are preliminary or of specialized interest, e.g., quick release reports, working papers, and bibliographies that contain minimal annotation. Does not contain extensive analysis.

- CONTRACTOR REPORT. Scientific and technical findings by NASA-sponsored contractors and grantees.

- CONFERENCE PUBLICATION. Collected papers from scientific and technical conferences, symposia, seminars, or other meetings sponsored or cosponsored by NASA.

- SPECIAL PUBLICATION. Scientific, technical, or historical information from NASA programs, projects, and mission, often concerned with subjects having substantial public interest.

- TECHNICAL TRANSLATION. English-language translations of foreign scientific and technical material pertinent to NASA's mission.

Specialized services that complement the STI Program Office's diverse offerings include creating custom thesauri, building customized databases, organizing and publishing research results…even providing videos.

For more information about the NASA STI Program Office, see the following:

- Access the NASA STI Program Home Page at ***http://www.sti.nasa.gov***

- E-mail your question via the Internet to help@sti.nasa.gov

- Fax your question to the NASA Access Help Desk at (301) 621-0134

- Telephone the NASA Access Help Desk at (301) 621-0390

- Write to:
  NASA Access Help Desk
  NASA Center for AeroSpace Information
  7121 Standard Drive
  Hanover, MD 21076-1320

NASA/TM-2000-209014

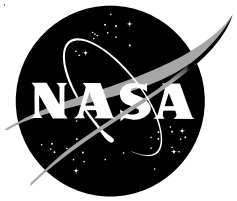

Design and Evaluation of a New Boundary-Layer Rake for Flight Testing

Trong T. Bui and David L. Oates
NASA Dryden Flight Research Center
Edwards, California

Jose C. Gonsalez
Dynacs Engineering Co., Inc.
Brookpark, Ohio

National Aeronautics and
Space Administration

Dryden Flight Research Center
Edwards, California 93523-0273

January 2000

DESIGN AND EVALUATION OF A NEW BOUNDARY-LAYER RAKE FOR FLIGHT TESTING

Trong T. Bui* and David L. Oates†
NASA Dryden Flight Research Center
Edwards, California

Jose C. Gonsalez‡
Dynacs Engineering Co., Inc.
Brookpark, Ohio

Abstract

A new boundary-layer rake has been designed and built for flight testing on the NASA Dryden Flight Research Center F-15B/Flight Test Fixture. A feature unique to this rake is its curved body, which allows pitot tubes to be more densely clustered in the near-wall region than conventional rakes allow. This curved rake design has a complex three-dimensional shape that requires innovative solid-modeling and machining techniques. Finite-element stress analysis of the new design shows high factors of safety. The rake has passed a ground test in which random vibration measuring 12 *g* rms was applied for 20 min in each of the three normal directions. Aerodynamic evaluation of the rake has been conducted in the NASA Glenn Research Center 8 × 6 Supersonic Wind Tunnel at Mach 0–2. The pitot pressures from the new rake agree with conventional rake data over the range of Mach numbers tested. The boundary-layer profiles computed from the rake data have been shown to have the standard logarithmic-law profile. Skin friction values computed from the rake data using the Clauser plot method agree with the Preston tube results and the van Driest II compressible skin friction correlation to approximately ±5 percent.

Nomenclature

Acronyms

ESP	electronically scanned pressure
FOS	factor of safety
FTF	Flight Test Fixture
LSWT	9 × 15 Low-Speed Wind Tunnel
OD	outer diameters
SWT	8 × 6 Supersonic Wind Tunnel

Symbols

B	logarithmic-law constant, $B = 5$
$\bar{C}_f$	skin friction coefficient transformed into the incompressible plane by the van Driest II transformation
g	gravitational acceleration constant, 32.2 ft/sec^2
M	Mach number
P	pressure
$\overline{Re}_\theta$	Reynolds number based on the boundary-layer momentum thickness transformed into the incompressible plane by the van Driest II transformation
rms	root-mean-square
T	temperature
U	stream-wise velocity
U^+	$\frac{u_{eq}}{u_\tau}$
u_{eq}	van Driest effective velocity

*Aerospace Engineer. Member AIAA.
†Aerospace Engineering Technician.
‡Wind-Tunnel Test Engineer. Member AIAA.

u_τ	wall friction velocity, $u_\tau = \sqrt{\frac{\tau_w}{\rho_w}}$
y	normal distance from the wall
y^+	distance in wall units, $y^+ = \frac{\rho_w u_\tau y}{\mu_w}$
κ	logarithmic-law constant, $\kappa = 0.41$
μ	viscosity coefficient
ρ	density
τ	shear stress

Subscripts

aw	adiabatic-wall conditions
conv	conventional rake used in wind-tunnel testing
e	edge of boundary layer
new	new rake
pitot	pitot tube readings
tunnel_total	wind-tunnel total conditions
w	wall conditions

Introduction

A new boundary-layer rake has been designed and built for flight testing on the F-15B/Flight Test Fixture (FTF).[1] The F-15B/FTF is an aerodynamics and fluid dynamics research test bed at NASA Dryden Flight Research Center (Edwards, California). Figure 1 shows the F-15B/FTF in flight; the FTF is the black, vertical, fin-like shape mounted on the centerline of the F-15B lower fuselage. Primarily made of composite materials, the FTF was designed for flight research at Mach numbers to a maximum of Mach 2.0.

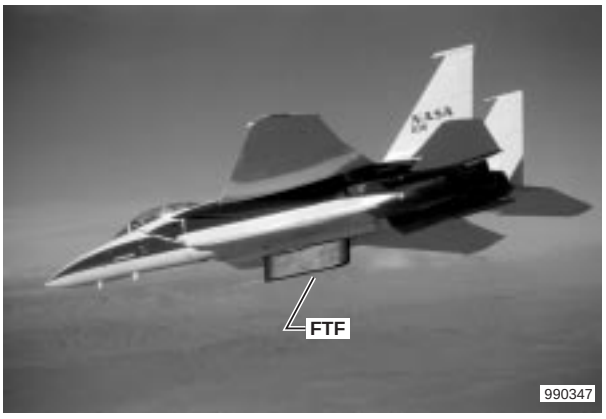

Figure 1. NASA Dryden F-15B/FTF in flight.

The new boundary-layer rake has been designed for the in-flight evaluation of skin friction gages. In this upcoming experiment, the skin friction gages will be mounted on the surface of the FTF together with the boundary-layer rake and a Preston tube. The flight conditions will be chosen so that the flow over the FTF approximates simple flat-plate flow, allowing good estimates of the skin friction to be obtained using the Clauser plot method[2] and the Preston tube method.[3] These estimates will then be used to evaluate the performance of the skin friction gages in flight.

To determine the boundary-layer momentum thickness, high-resolution survey of the turbulent boundary layer is needed. Also, the Clauser plot method requires a good clustering of probes in the logarithmic-law region. The new boundary-layer rake has been designed to satisfy these requirements. A feature unique to this rake is its curved rake body, which allows the pitot tubes to be more densely clustered in the near-wall region than current rakes allow. The new rake is also more compact than existing canted rake designs.

This paper provides a description of the new rake design. The solid-modeling and machining techniques used in the fabrication of this new rake are also described. Finite-element stress analysis and ground vibration test results are discussed. To evaluate the aerodynamics characteristics of the rake, a wind-tunnel test has been conducted in the NASA Glenn Research Center (Cleveland, Ohio)[§] 8 × 6 Supersonic Wind Tunnel (SWT) at Mach numbers ranging from Mach 0 to Mach 2. Representative wind-tunnel test results are provided.

Note that use of trade names or names of manufacturers in this document does not constitute an official endorsement of such products or manufacturers, either expressed or implied, by the National Aeronautics and Space Administration.

Rake Design and Fabrication Technique

The design of the new, curved, boundary-layer rake resulted from considering different configurations (fig. 2). The rakes in this figure are shown as viewed from an upstream, edge-on position.

Rake A is a conventional, vertical design that has been extensively used in wind-tunnel and flight testing. Probes can not be clustered too closely in the near-wall

[§]Formerly NASA Lewis Research Center.

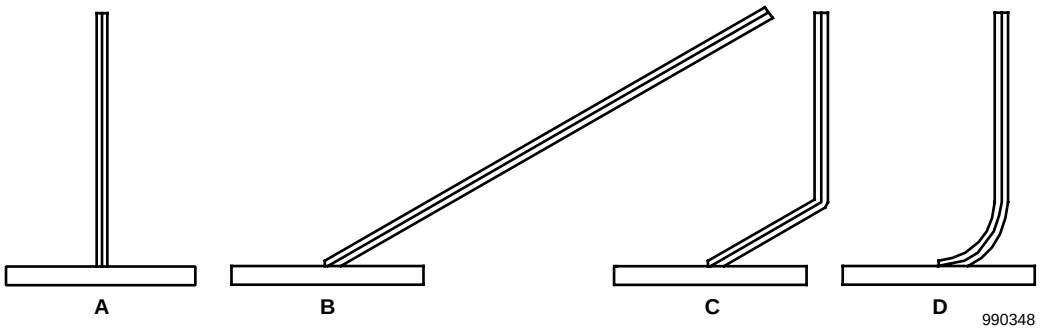

Figure 2. Rake designs considered.

region of this rake design because of interference effects; therefore, the rake resolution in the near-wall region could be insufficient. Rake B was designed to overcome this problem. This rake is canted at an angle to the surface, which allows smaller probe spacing in the vertical direction near the wall than rake A allows. The major drawbacks of this approach are that the boundary layer is assumed to be uniform over a large span-wise region, and that the canted rake requires additional room to install and interferes with or obscures other instrumentations nearby. As an example, the canted rake that has been used on the FTF covers as much as 5 in. in the span-wise direction.

A new semicanted rake design, rake C, was considered in which the canted portion covers only the near-wall region and the rake becomes vertical away from the wall where the tight probe spacing is not needed. This design retains the desirable probe clustering feature of rake B in the near-wall region but is much more compact in the span-wise direction. Unfortunately, the sharp angles in the rake C design present manufacturing and structural problems.

Rounding out the sharp angles in rake C led to the rake D design. The curved lower portion of rake D allows tighter probe clustering in the vertical direction than was possible with the canted rakes. The lower portion is smoothly blended into the vertical upper portion of the rake, resulting in a compact rake with very good probe clustering characteristics in the near-wall region.

Note that the pitot probes in rakes B–D are distributed over a distance in the span-wise direction. These rake designs should be used only when the boundary layer is expected to be homogeneous in the span-wise direction.

Several possible design variations exist to rake D. Total pressure probes can be replaced by other sensors, such as total temperature probes, that will allow a distribution of fluid dynamic properties other than total pressures to be measured. The circular arc in the curved portion of the rake can be replaced by other geometrical shapes (parabola, hyperbola, and so forth) to allow more control in the degree of probe clustering in the near-wall region. Additionally, a second curved section can be used above the rake. This modification will allow probes to be tightly clustered at both of the upper and lower ends of the rake, thereby resolving both boundary layers at the two solid walls in the flow (for example, internal fluid flows in inlets, ducts, and nozzles).

New Rake Design

Figure 3 shows a three-view engineering drawing of the new rake design. The new rake consists of a horizontal rake pedestal, a vertical probe support, and an array of total pressure probes. The rake pedestal is mounted flush with the surface to be surveyed. The vertical probe support consists of a curved lower portion and a straight vertical upper portion. An array of total pressure probes is mounted along the upstream edge of the vertical probe support.

Current analysis of boundary-layer velocity profiles on the FTF collected during past F-15B flight tests[1] shows that the logarithmic-law region extends approximately 0.5 in. above the surface of the FTF. As a result, the probes are spaced on the curved portion of the new rake such that approximately ten probes are located in the first 0.5 in., spaced approximately two probe outer diameters (OD) apart. The remaining probes on the rake are spaced approximately 3.75 OD apart. These spacings will provide good probe clustering in the logarithmic-law region and give good coverage for the entire FTF turbulent boundary layer.

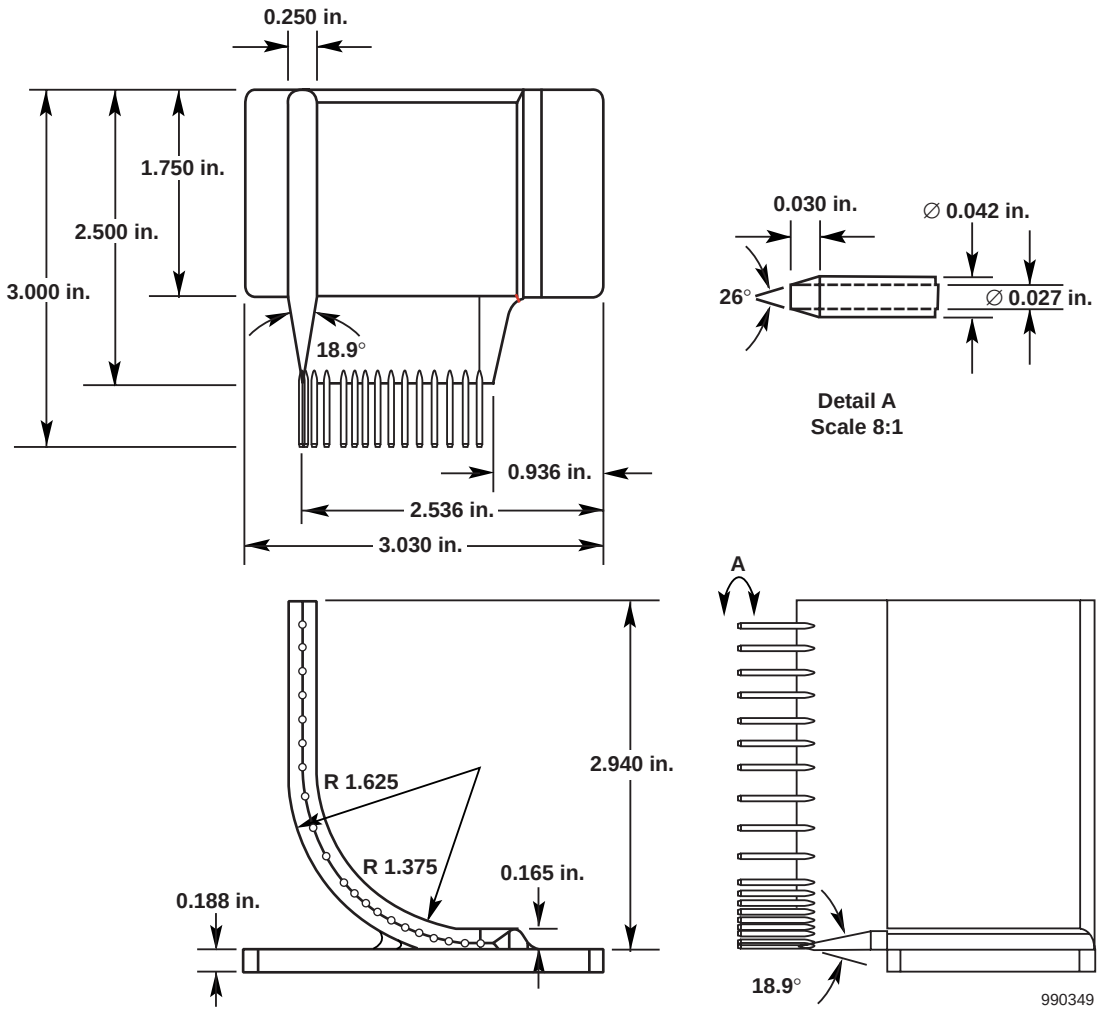

Figure 3. Detailed three-view drawing of the new curved rake design.

Gracey has reported that the total pressure reading from a pitot probe is sensitive to large local flow angles.[4] To minimize this sensitivity and obtain good total pressure measurements for a wide range of flow angles, the tips of the probes can be internally or externally chamfered. Data previously reported[4] show that pitot probes with square cut tips are insensitive to local flow angles of a maximum of ±11°. For pitot probes with a 30-deg conical (externally chamfered) tip, the range of insensitivity increases to ±17.5°, and a 15-deg conical tip has an even larger range of insensitivity of ±21°. The tips of the probes on the new rake are chamfered on the outside, resulting in a 26-deg conical tip. This new rake is expected to be insensitive to local flow angles of less than ±17.5°.

Another important consideration for pitot probes is the probe centerline displacement effect. When a simple pitot probe is used in the presence of a total pressure gradient, the indicated total pressure does not represent the pressure that exists on the centerline of the tube, but a slightly higher value. This effect can be interpreted as the effective centerline of the tube being displaced from the geometric center toward the direction of higher total pressure. Reference 5 provides a comprehensive survey of literature regarding work in this area. The offset distance can be as large as 0.18 OD for large pitot tubes with square-cut tips; however, the displacement effect can be quite small (less than 0.02 OD) for small pitot tubes with conical tips such as those used in the present rake. Having an outer diameter of 0.042 in. and a conical tip, the centerline displacement error for the pitot probes of the new rake is expected to be less than 0.00084 in. This error is well within the uncertainty of the actual probe locations.

The thickness of the vertical probe support was chosen to be 0.25 in. based on an existing rake that had

been used on the F-15B airplane. Gettelman and Krause found that the pitot probe support could interfere with the probe reading.[6] This interference effect is reduced as the distance between the probe tip and probe support is increased, and asymptotes to a minimum value for the ratios of probe length to probe support thickness greater than 3. In the new rake, the probe tip is located 1.75 in. upstream of the maximum thickness location of the support, giving a ratio of pitot probe length to support thickness of 5.

Rake Fabrication Techniques

Although the curved rake concept described above is quite simple, the mechanical design and fabrication of the actual hardware were very challenging. The three-dimensional design consists of a large number of curves and angles. In addition, the actual rake needs to be rugged to withstand supersonic wind-tunnel and aircraft operation, and provisions need to be made for routing and installing the pitot tubes. Consequently, innovative three-dimensional–solid-modeling and machining techniques were required.

Starting from a three-view conceptual sketch, a three-dimensional solid model was constructed using three-dimensional–solid-modeling software. The same software was used throughout the entire design and machining process, ensuring accurate machining of the rake from the three-dimensional solid model. The actual rake body needed to be strong and streamlined, and provisions had to be made for the installation and routing of the stainless-steel pitot tubes.

After a solid model was created, a computer-controlled electrical discharge machine was used with a 0.010-in. wire to cut the basic shape of the rake body out of a solid block of aluminum alloy 2024-T351. (The residual piece of aluminum with the outside contour of the rake was saved and used as a fixture for the rake during subsequent machining work.) The rake was then machined on a computer–numerically controlled milling machine. First, the rake pedestal was machined for flush mounting on a flat surface. To make room for the installation of the pitot tubes, a cavity was machined in several steps inside the rake body. Then, mounting holes for the pitot tubes were drilled on the rake leading edge, and the leading edge was tapered to an angle of 18.9°. To close off the cavity in the rake body, an aluminum rake cover was created using the wire electrical discharge machine.

The pitot tubes used in the rake were fabricated from T304 stainless-steel tubing (0.042-in. outer diameter and 0.0075-in. nominal-wall thickness, annealed to one-half hard condition). As discussed in the New Rake Design section, the tips of the pitot tubes were chamfered on the outside to reduce their sensitivity to local flow angles. Then the probes were inserted into the rake body. A low-viscosity, single-component, anaerobic, methacrylate ester adhesive, Loctite® 609[¶] was used to hold the pitot tubes in place inside the rake body. To cushion the pitot tubes and protect them from vibration during flight, room-temperature–vulcanizing silicone rubber was applied to the inside of the rake cavity.

Figure 4 shows the finished rake. The surface of the rake body was anodized to help protect it from corrosive effects during high-speed–aircraft and wind-tunnel operation. Figure 4(a) shows the rake with the cover on. Figure 4(b) shows the rake with the cover off; installation and routing inside the rake of the pitot tubes can be seen in this view.

EC 98 44775-04

(a) Rake with cover on.

Figure 4. The new, curved, boundary-layer rake.

[¶]Loctite Corporation, Rocky Hill, Connecticut.

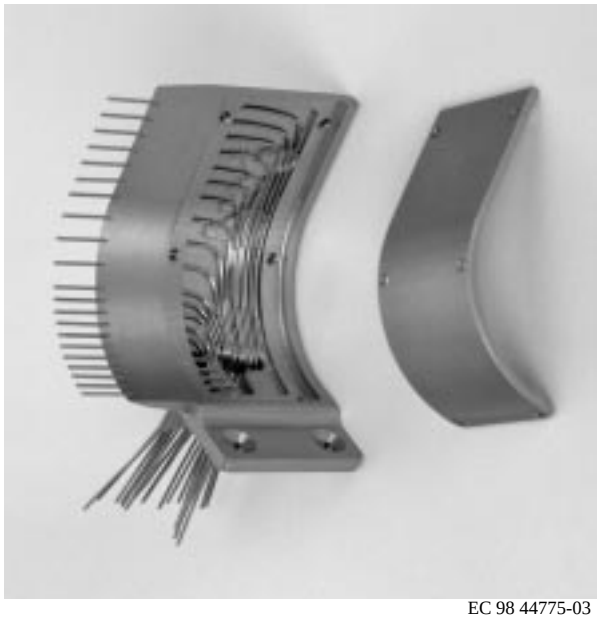

EC 98 44775-03

(b) Rake with cover off.
Figure 4. Concluded.

Flight Qualification Analysis and Testing

To determine the structural integrity of the new rake, finite-element stress analysis was conducted for both wind-tunnel and aircraft operations. Factors of safety were computed from the solutions of the finite-element analysis. Also, a ground vibration test on the rake was conducted at NASA Dryden.

Finite-Element Stress Analysis

To qualify the rake for supersonic wind-tunnel operation, the computer solid model was analyzed using the COSMOS/Works™[#] finite-element analysis package. Inviscid flow theory was used to obtain the pressure distribution on the rake body. In the finite-element analysis, the pressures were specified as boundary conditions while the base of the rake was held rigidly fixed. The static stress analysis was conducted using the fast finite-element (FFE) solver option in COSMOS/Works™. This fast, robust, and accurate finite-element solver provides solutions significantly faster than standard finite-element direct solvers. The finite-element mesh used in the analysis was automatically generated by COSMOS/Works™ using the default high-quality meshing option.

The factor of safety (FOS), based on the maximum von Mises stress, was computed for subsonic, transonic, and supersonic wind-tunnel test conditions (with no sideslip) from the solutions of the finite-element analysis. Table 1 shows a summary of the results.

Table 1. Minimum factors of safety for wind-tunnel test conditions.

Mach number	Factor of safety
2.0	26
1.8	21
1.6	17
1.4	11
1.2	13
0.9	26
0.6	42
0.4	98

The stress on the rake is most severe in the transonic Mach number range. This severe stress is caused by high pressure from the detached normal shock wave at the rake leading edge. The minimum FOS ranges from approximately 10 for transonic Mach numbers to approximately 100 for low subsonic Mach numbers. As expected, no structural problems with the rake were found during the actual supersonic wind- tunnel test.

A similar stress analysis was done for straight and level flight conditions for the F-15B/FTF. Table 2 shows a summary of the results. Altitudes from sea level to 45,000 ft were considered at 5,000 ft intervals. At each altitude, the maximum flight Mach number obtained from the F-15B/FTF flight envelope[1] was used to calculate the aerodynamic loads and the structural stresses on the rake.

The FOS ranged from 12 at Mach 1 and an altitude of 10,000 ft to 37 at Mach 2 and an altitude of 45,000 ft. Because of the high FOS, the rake is expected to survive F-15B/FTF straight and level flight operation throughout the entire flight envelope. The side loads on the rake and new factors of safety will need to be determined for flight tests with large angles of attack or sideslip.

[#]Structural Research & Analysis Corporation, Los Angeles, California.

Table 2. Minimum factors of safety for F-15B/FTF straight and level flight conditions.

Altitude, ft	Mach number	Factor of safety
0	0.907	16
5,000	0.979	17
10,000	1.057	12
15,000	1.143	12
20,000	1.242	12
25,000	1.356	12
30,000	1.489	13
35,000	1.646	25
40,000	1.829	31
45,000	2.038	37

Ground Vibration Test

Flight equipment on the F-15B/FTF is required at NASA Dryden to be tested to worst-case operating conditions. As part of this requirement, a ground vibration test was conducted on the rake. In this test, the rake was securely mounted on a vibration table and random vibration measuring 12 g rms was applied for 20 min in each of the three normal directions. The frequency for the vibration test ranged from 15 to 2000 Hz. Accelerometers were affixed to the mounting fixture and the side of the rake to document the acceleration on the rake. The rake passed the ground vibration test with no anomalies.

Wind-Tunnel Testing of the Rake

To evaluate the aerodynamic performance of the new rake design, two different boundary-layer rakes were separately tested in two wind-tunnel tests: the new, curved rake and a rake representative of a conventional design. The wind-tunnel tests were conducted in the NASA Glenn SWT. The first test used the new curved rake; the second test, which took place one week later, used the conventional rake. The conventional rake was used as a check for the new rake. Nearly identical wind-tunnel flow conditions were used for both tests. Both of the tests were conducted for Mach numbers ranging from 0.05 to 2.00.

Description of Facility

Figure 5 shows a plan view of the SWT and 9 × 15 Low-Speed Wind Tunnel (LSWT) complex. The SWT is an atmospheric tunnel with Mach number capabilities ranging from 0.0 to 0.1 and 0.25 to 2.0. The test section has two parts: a solid-wall section and a porous-wall section. The forward 9-ft, 1-in. section is the solid-wall supersonic test section. The downstream 14-ft, 5-in. section is the porous-wall transonic test section.

The test section is housed in a vacuum chamber. During tunnel operation, the vacuum chamber provides bleed to the transonic test section through the porosity

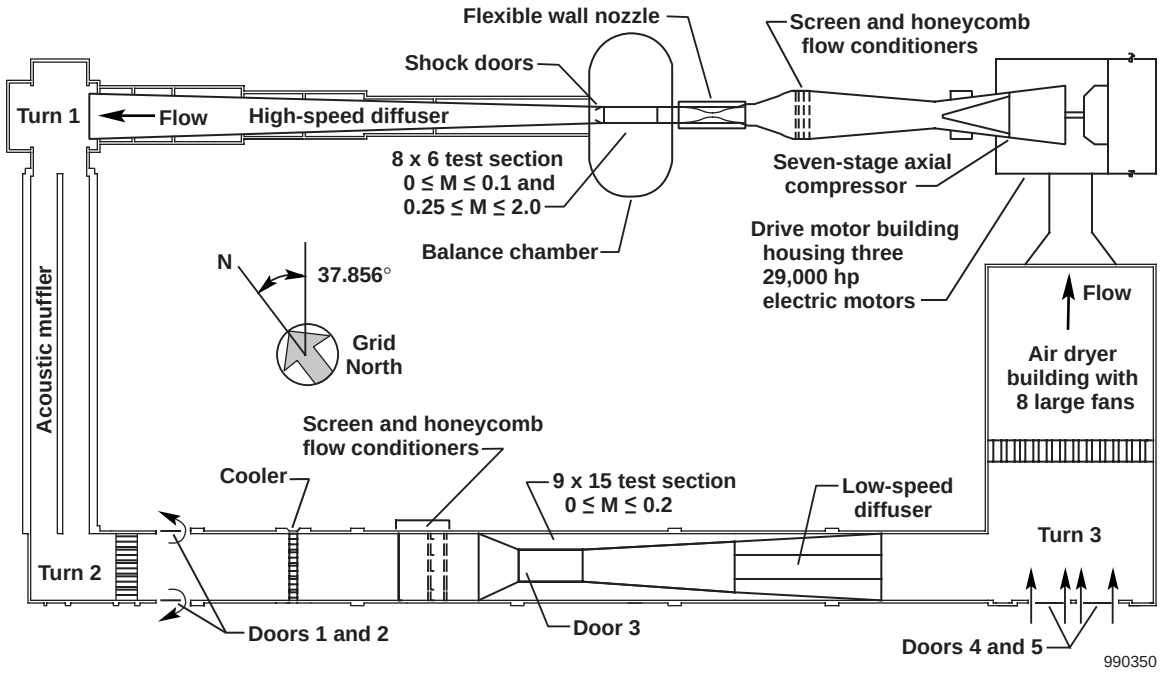

Figure 5. Plan view of the NASA Glenn SWT and LSWT complex.

holes. This bleed allows regulation of the static pressure in the test section. During the rake tests, the wall pressure gradient in the stream-wise direction at the rake location was found to be negligible for most cases.

The SWT can be run in two modes. In the aerodynamic, or closed-loop, mode, air is continually recirculated through the tunnel loop. In the propulsion, or open-loop, mode, air is drawn in through doorways 4 and 5 and exhausted through doorways 1 and 2 (fig. 5). Door 3, which is directly at the entrance of the LSWT (fig. 5), is closed. Because air bypasses the LSWT in the open-loop mode, model work can occur in the LSWT while the SWT operates.

During the tests described here, the boundary-layer rakes were installed on the ceiling and in the supersonic solid-wall portion of the SWT test section. The SWT operated in propulsion, or open-loop, mode.

Test Hardware

Figures 6 and 7 show installation photographs of the two rakes. Also seen in these photographs is the 0.125-in. outer diameter Preston tube, mounted side by side with the rakes. The outer diameter of the Preston tube was chosen specifically for the F-15B test conditions.[7] (Full three-view drawings of the new rake and the representative conventional rake are shown in figures 3 and 8, respectively.) Table 3 shows pitot probe heights for both rakes.

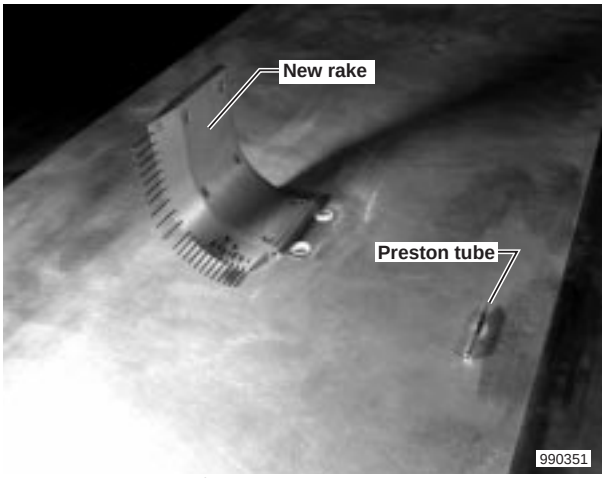

(Original photo courtesy of NASA Glenn Research Center)

Figure 6. Installation photograph of the new rake and Preston tube in the SWT.

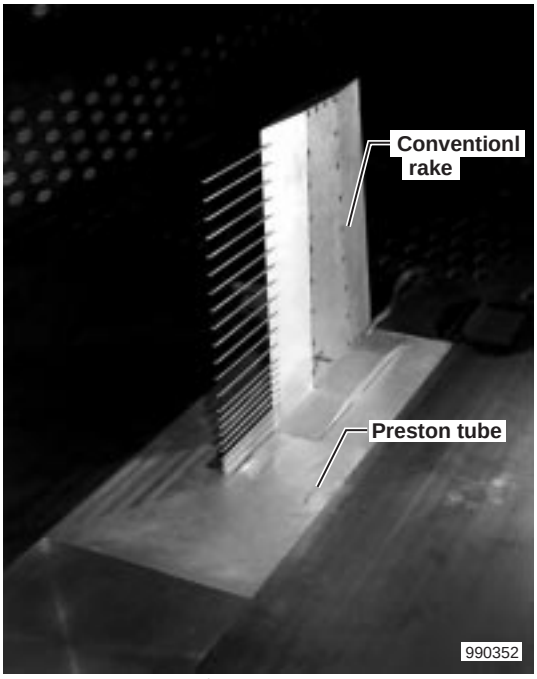

(Original photo courtesy of NASA Glenn Research Center)

Figure 7. Installation photograph of the representative conventional rake and Preston tube in the SWT.

Many notable differences exist between the two rakes. The new rake is curved, whereas the conventional rake is vertically straight. Pitot tube outer diameters for the new and conventional rakes are 0.042 and 0.188 in., respectively. Pitot tube lengths are 0.5 and 6.0 in. for the curved and conventional rakes, respectively. The curved rake pitot tube tips have external chamfers; the conventional rake pitot tube tips have internal chamfers, or countersinks. The overall height of the new rake is 2.94 in.; the overall height of the conventional rake is 18.5 in.

Each rake was positioned on the ceiling of the SWT in the forward, solid-wall portion of the supersonic test section. The axial location of the pitot tube tips was 83.4 in. downstream of the tunnel zero station (fig. 9). Each rake was centered along the tunnel centerline in the span-wise direction. (The curved rake was centered in the span-wise direction with respect to its mounting plate.)

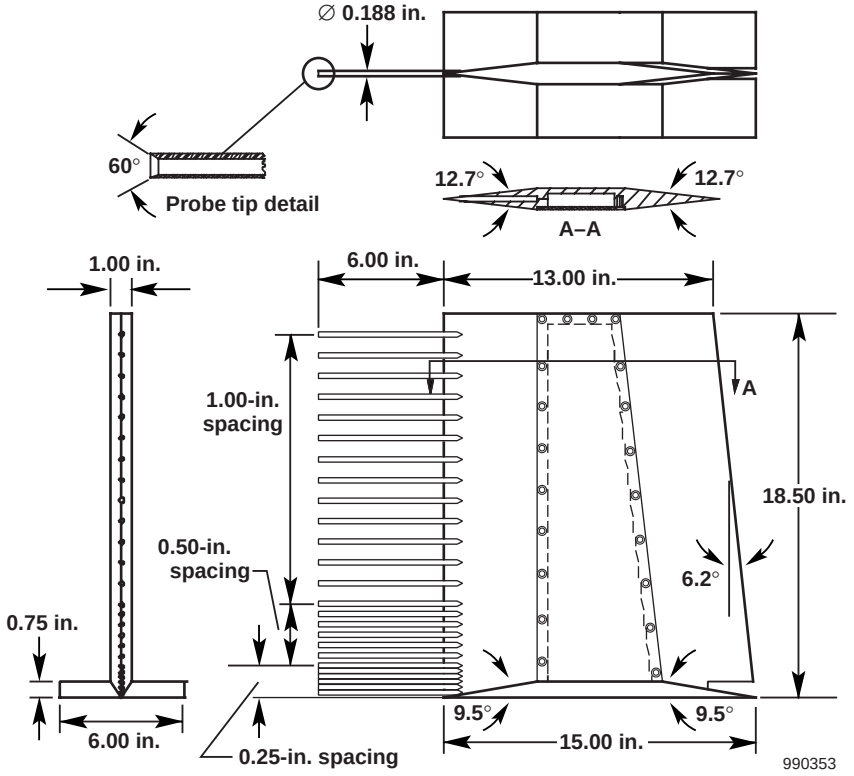

Figure 8. Detailed three-view drawing of the representative conventional boundary-layer rake.

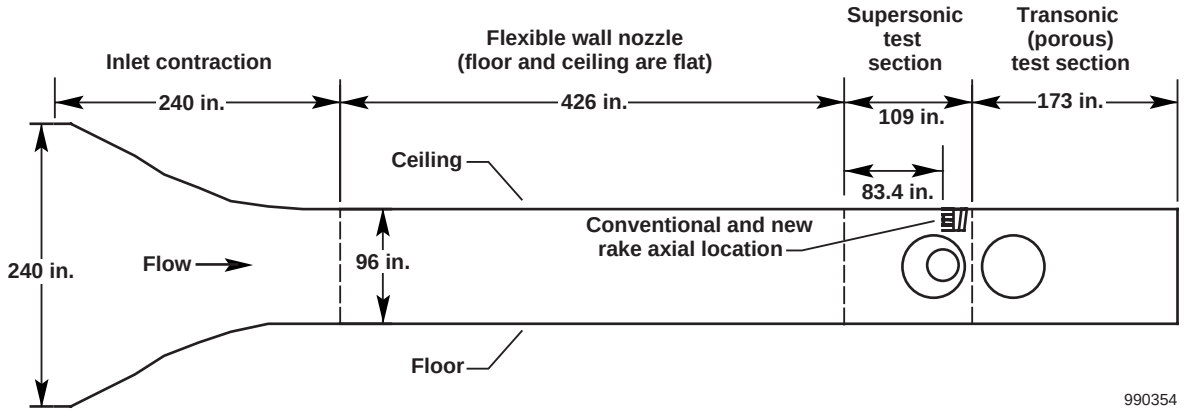

Figure 9. Elevation of the SWT inlet contraction, flexible wall nozzle, and test section showing the axial location of the new and conventional boundary-layer rakes.

Table 3. Probe heights for the boundary-layer rakes.

Probe	Probe height, in.	
	New rake	Conventional rake
1	0.0400	0.25
2	0.0457	0.50
3	0.0628	0.75
4	0.0911	1.00
5	0.1305	1.25
6	0.1805	1.50
7	0.2410	2.00
8	0.3113	2.50
9	0.3909	3.00
10	0.4793	3.50
11	0.5758	4.00
12	0.7900	4.50
13	1.0270	5.50
14	1.2795	6.50
15	1.5400	7.50
16	1.7400	8.50
17	1.9400	9.50
18	2.1400	10.50
19	2.3400	11.50
20	2.5400	12.50
21	2.7400	13.50
22	N/A	14.50
23	N/A	15.50
24	N/A	16.50
25	N/A	17.50

The Preston tube, which has an inner-diameter–to–outer-diameter ratio of 0.584, was installed at the same axial location as the boundary-layer rakes. Figure 10 shows the location of the Preston tube as well as the locations for surface temperature thermocouples and static pressure taps. The thermocouples and pressure taps were used to provide local wall temperature and static pressure data needed in the boundary-layer analysis. Type “E” or nickel-chromium and copper-nickel welded thermocouple-junctions were “potted” into two 0.125-in.–diameter “through holes” in the tunnel ceiling at the locations shown in figure 10. The potting material used was an electrically nonconductive epoxy that allows the thermocouple-junction to sense the wall surface temperature without electrically affecting the junction.

Alongside each surface temperature thermocouple was a 0.032-in.–diameter static pressure tap. One surface thermocouple and one static pressure tap were located at axial station 83.4 in. The other thermocouple and static tap were located 3.0 in. upstream. The locations of the Preston tube, surface thermocouples, and static pressure taps were selected to minimize possible aerodynamic disturbances from the boundary-layer rakes.

Instrumentation and Data Acquisition

Two instrumentation systems were used to measure the pressures and temperatures for this wind-tunnel test: an electronically scanned pressure (ESP) system and an isothermal thermocouple-junction reference block.

All pressures including the boundary-layer rake pitot pressures, the wall static pressures, and the wind-tunnel total and static pressures were measured using the ESP system. The ESP system was configured with a 30-lbf/in^2 absolute pressure calibration unit and ±15-lbf/in^2 differential pressure modules. The resolution of the system was configured to be 1000 counts/(lbf/in^2).

The master pressure calibration unit in the ESP system had a 30-lbf/in^2 absolute high-accuracy pressure transducer. The system uses atmospheric pressure as its reference pressure. Typical atmospheric pressure at NASA Glenn is 14.4 lbf/in^2 absolute. The system automatically calibrates itself every hour, or the test engineer can initiate a system calibration (for example, at the beginning of a data acquisition sweep). During a calibration, solenoid valves send predetermined pressures to each pressure port of every pressure module.

For this test, the calibration pressures are 2.4, 8.4, 14.4, 21.9, and 29.4 lbf/in^2 absolute, which convert to –12.0, –6.0, 0.0, 7.5, and 15.0 lbf/in^2 gauge if the atmospheric pressure is 14.4 lbf/in^2 absolute. The absolute pressure transducer in the pressure calibration unit accurately measures these five individual

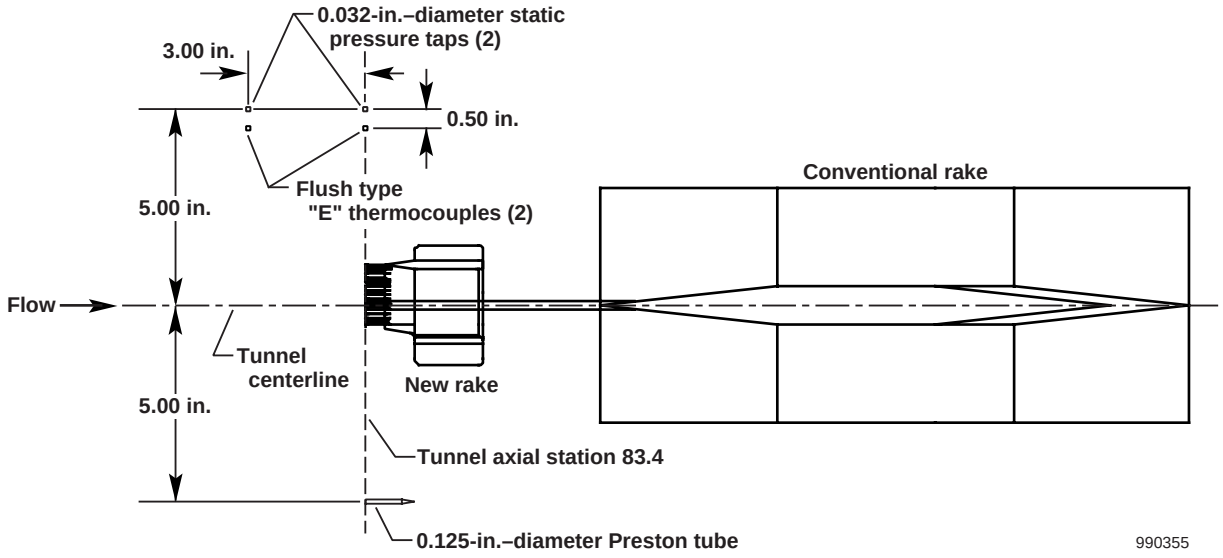

Figure 10. Top view of Preston tube, surface temperature thermocouple, and static pressure tap locations with respect to the new and conventional rakes, superimposed in this figure for illustrative purpose only, and tunnel centerline.

calibration pressures, which are applied to all of the pressure ports in the modules. The system constructs calibration curves for every single port of every single module. The ±15 lbf/in^2 differential modules have a measurement range of approximately 0–29.4 lbf/in^2 absolute for an atmospheric reference of 14.4 lbf/in^2 absolute. The pressure calibration unit also monitors the atmospheric reference pressure. If the atmospheric pressure changes, the transducer in the pressure calibration unit will sense it and correct the pressure data automatically.

All temperatures, including the wall surface temperatures and the wind-tunnel total temperatures, were measured using the isothermal thermocouple-junction reference block. The thermocouple voltages from the reference block were digitized using a NEFF Model 620 Series 400[**] multiplexed 16-bit analog-to-digital converter. The input voltage for the thermocouple channels was 0–5 mV.

Data acquisition was carried out by a Digital Alpha server model 2100[††] running the standard NASA Glenn data acquisition software. This software retrieved the pressure data from the ESP system and the voltage data from the NEFF analog-to-digital converter and converted these data into engineering units. This software allowed the data to be recorded and displayed on computer screens in either graphical or numerical formats at an update rate of 1/sec.

All pressures measured during this test, including the boundary-layer rake and wind-tunnel facility pressures have an uncertainty of ±0.006 lbf/in^2 absolute (±0.03–0.2 percent). All temperatures measured during this test, including surface temperature and wind-tunnel total temperatures, have an uncertainty of ±2.3 °F (±0.4 percent).

Test Conditions

During the test, the tunnel total temperature ranged from 630 °R (at Mach 2.0) to 500 °R (at Mach 0.05). The tunnel total pressure ranged from 25 lbf/in^2 absolute (at Mach 2.0) to 14 lbf/in^2 absolute (at Mach 0.05).

For each test, approximately 4.0 hr were needed to collect all of the data, including 3.5 hr of main drive operation (Mach 0.25–2.00) and 0.5 hr using air dryer building fans (Mach 0.05–0.10). A complete sweep of Mach numbers, ranging from 0.05 to 2.00, was conducted in each test. Each data reading is an average of 20 data points. These data points were sampled at a rate of 1 sample/sec. Three readings were taken at each Mach number.

[**]NEFF Instrument Corporation, Monrovia, California.
[††]Compaq Computer Corporation, Houston, Texas.

Wind-Tunnel Rake Evaluation Results

Standard compressible turbulent boundary-layer relations[8] were used to compute the velocity profiles, momentum thickness, and Reynolds number based on momentum thickness from the wind-tunnel data at Mach numbers 0.3–2.0. A Mathcad®[‡‡] program was written to automate the data reduction process and the boundary analysis. To analyze the wind-tunnel data, the following steps were used:

1. The boundary-layer velocity profiles were computed from the rake pitot pressures.
2. The compressible turbulent boundary-layer velocity profiles were collapsed for Mach numbers from 0.3 to 2.0 using the van Driest effective velocity concept.[8]
3. The skin friction was predicted using the van Driest II skin friction correlation.[9]
4. The skin friction was computed using the Clauser plot method.[10]
5. The skin friction was computed using the Preston tube method.[11]
6. The skin friction results obtained from the Clauser plot and the Preston tube methods were compared with the van Driest II prediction.

Rake Pitot Pressure Profiles

Because most compressible turbulent boundary-layer theories assume adiabatic walls, figure 11 shows a plot of the ratio of the wall temperature (T_w) to the adiabatic-wall temperature (T_{aw}) of the wind-tunnel test. The wall temperature is approximately adiabatic for most flow conditions. The wind-tunnel test began with a slightly cold wall (T_w/T_{aw} = 0.96) at Mach 1.972. Toward the end of the test, the wall gets slightly hotter (T_w/T_{aw} = 1.02) at Mach 0.294.

Figures 12–15 show the pitot pressure profiles measured by the new rake and the conventional rake for boundary-layer–edge Mach numbers ranging from 0.294 to 1.972. Despite numerous differences in the physical rake designs, the results from both rakes agree for subsonic, transonic, and supersonic Mach numbers. The agreement is very good for Mach 0.294. At Mach numbers higher than 0.294, the pitot pressures from the conventional rake are slightly higher than the new rake in the near-wall region. This discrepancy will be examined more closely in the following section.

[‡‡]MathSoft, Inc., Cambridge, Massachusetts.

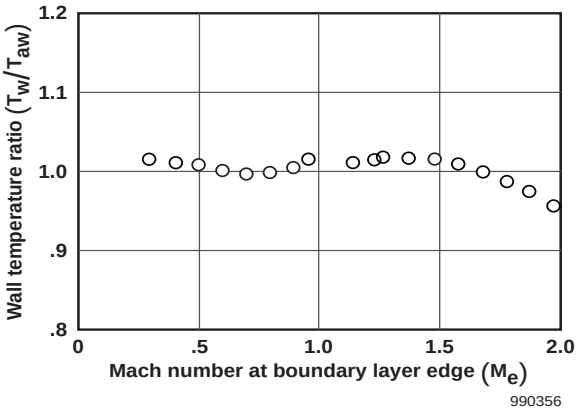

Figure 11. Wall temperature ratio at the rake location.

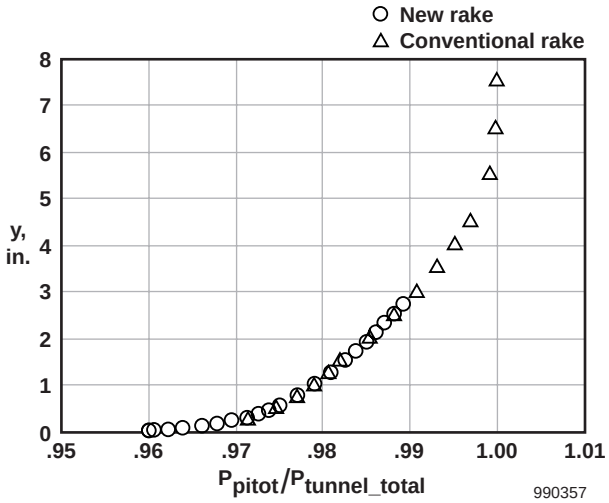

Figure 12. Boundary-layer pitot pressure profile, M_e = 0.294

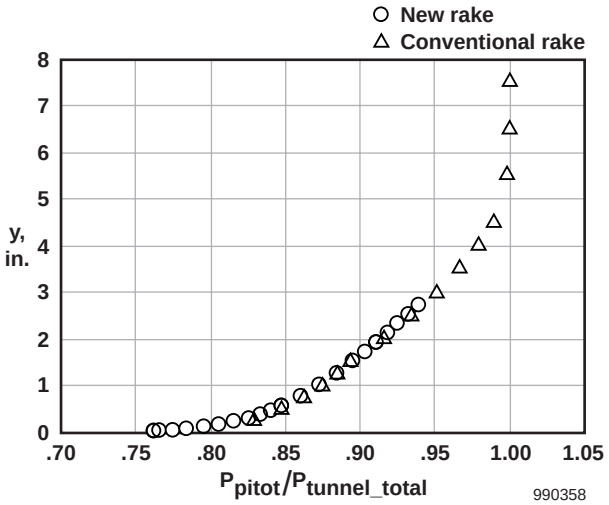

Figure 13. Boundary-layer pitot pressure profile, M_e = 0.794.

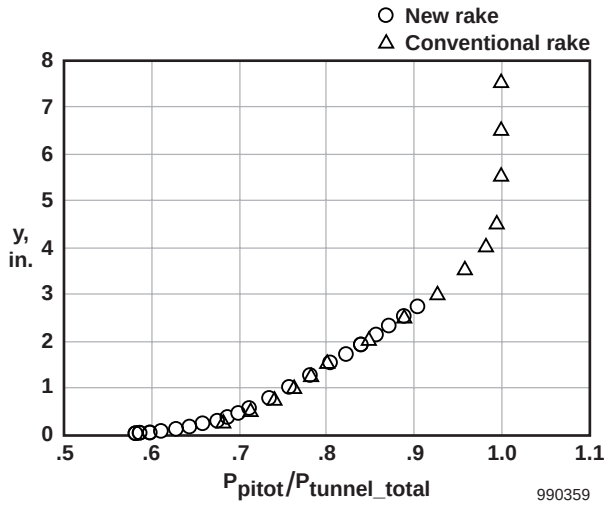

Figure 14. Boundary-layer pitot pressure profile, M_e = 1.139.

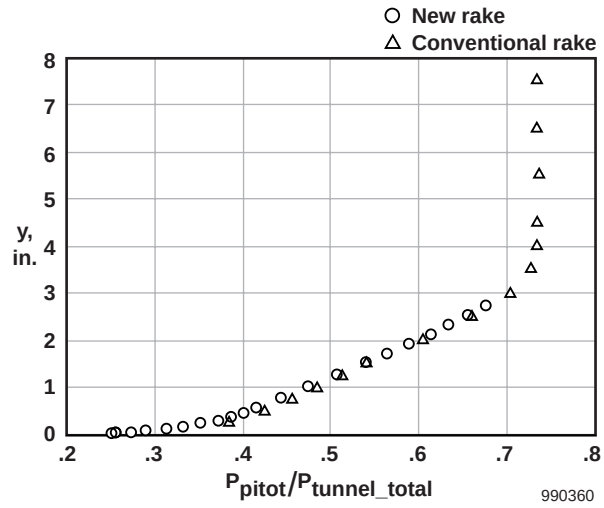

Figure 15. Boundary-layer pitot pressure profile, M_e = 1.972.

The boundary-layer thickness (at $\frac{U}{U_e}$ = 0.99) in the wind tunnel at the rake location ranges from 3.12 in. at Mach 1.972 to 5.03 in. at Mach 0.294. Because the new rake is only 2.94-in. high, it did not cover the full wind-tunnel wall boundary layer. Nevertheless, a full pitot pressure profile was required for the boundary-layer analysis.

As figures 12–15 show, the agreement between the two rakes is good, especially in the region away from the wall. Consequently, the pitot pressure ratios from the conventional rake were used to complete the new rake pitot pressure profiles in the boundary-layer analysis. At y locations lower than 2.94 in., the pitot pressures from the new rake were used. At y locations higher than 2.94 in., the pitot pressures were computed as follows:

$$(P_{pitot})_{new} = \left(\frac{P_{pitot}}{P_{tunnel\_total}}\right)_{conv} \times (P_{tunnel\_total})_{new}$$

The boundary-layer velocity profiles were computed from the combined pitot pressure profiles and the new rake wind-tunnel test conditions.

Wind-Tunnel Boundary-Layer Velocity Profiles

The van Driest effective velocity concept (as outlined in reference 8, page 544) was used to correlate the compressible turbulent boundary-layer velocity profiles for Mach numbers ranging from 0.294 to 1.972. Using this technique, the compressible boundary-layer velocity profiles at different free-stream Mach numbers can be collapsed into one curve and compared with the standard incompressible logarithmic-law velocity profile.

Figures 16–19 compare the turbulent boundary-layer velocity profiles in dimensionless wall units (y^+ and U^+) with the van Driest logarithmic law (shown as a straight line). The symbol U^+ is defined to be the van Driest effective velocity (u_{eq}) divided by the wall friction velocity (u_τ). The wall friction velocity was computed from the skin friction coefficient that was obtained using the Preston tube method and the Bradshaw-Unsworth[12] correlation. The logarithmic-law constants of κ = 0.41 and B = 5 are the standard incompressible values recommended in reference 8.

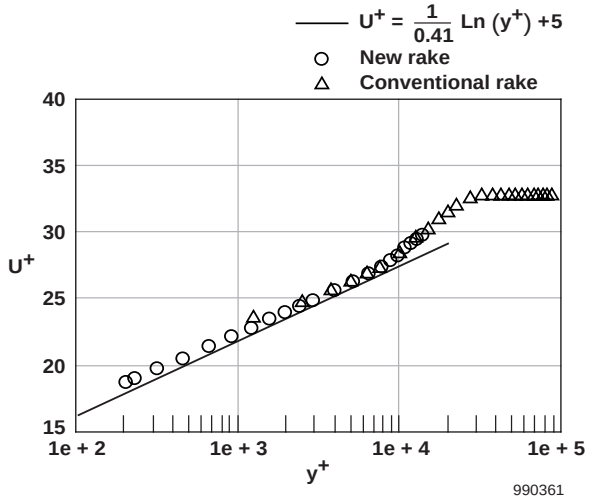

Figure 16. Boundary-layer velocity profile, M_e = 0.294.

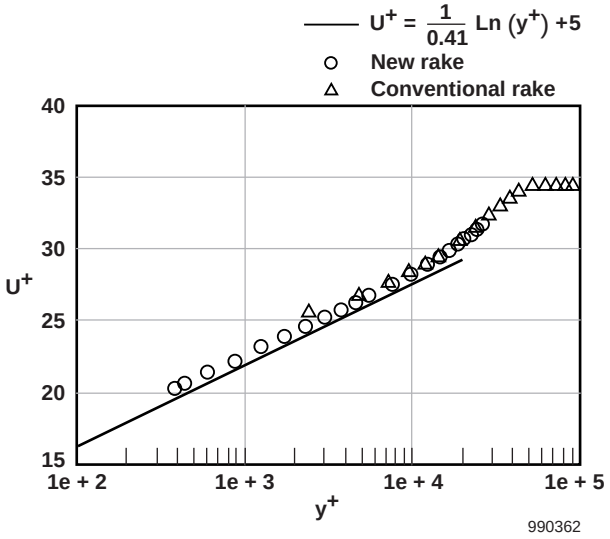

Figure 17. Boundary-layer velocity profile, M_e = 0.794.

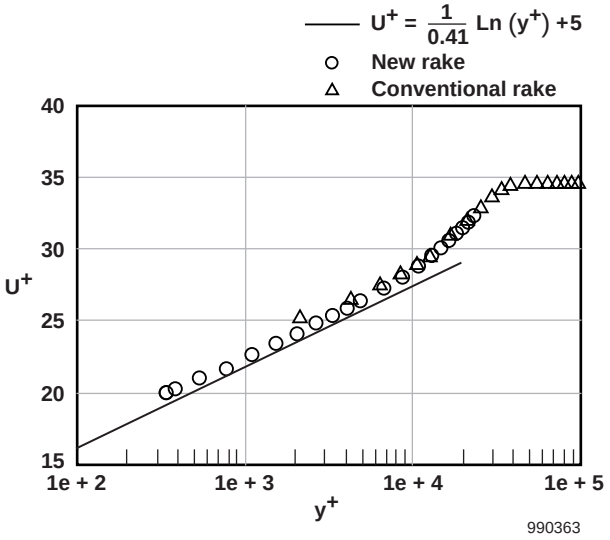

Figure 18. Boundary-layer velocity profile, M_e = 1.139.

The boundary-layer velocity profiles are seen to have the standard logarithmic profile for all Mach numbers. Although the slopes of the data in the linear logarithmic-law region match the van Driest logarithmic law well, U^+ values from both of the rakes are approximately 2.3–4.5 percent greater than the van Driest logarithmic-law line.

The data points from the new rake lie on a straight line in the logarithmic-law region. The slope of the new rake data also matches the slope of the standard logarithmic-law line. These observations give strong support that the new rake probes, including the ones closest to the wall, indicated the correct total pressure values. The new rake provides good resolution of the logarithmic region, and the data blend smoothly into the boundary-layer–wake region. The first data point off the wall has a y^+ value of approximately 200 to 300. The large number of data points in the linear logarithmic-law region is helpful for calculating the boundary-layer skin friction with the Clauser plot method.

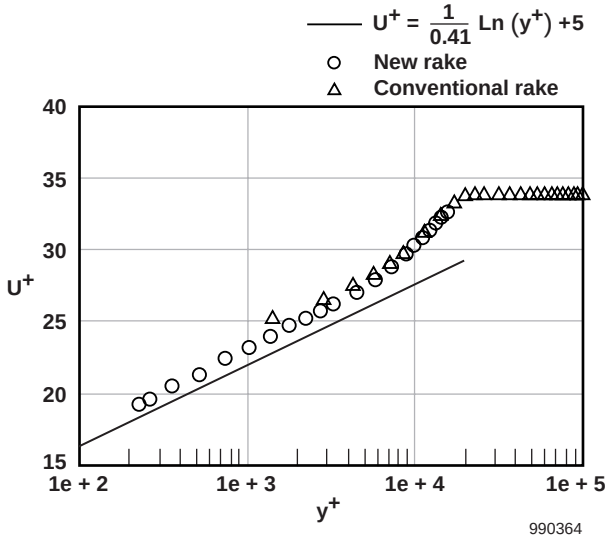

Figure 19. Boundary-layer velocity profile, M_e = 1.972.

The conventional rake data points closest to the wall are noticeably higher than the new, curved rake data. Additionally, the conventional rake data points depart from the slope of the standard logarithmic-law line. This discrepancy is caused by the high total pressure indications by the conventional rake observed in the Rake Pitot Pressure Profiles section. Because the conventional rake uses larger pitot probes than the new rake does and the total pressure readings are toward the high side, the first few probes of the conventional rake might be susceptible to the problem of probe centerline displacement effect mentioned in the New Rake Design section.

Skin Friction Results

The skin friction values were calculated using the following four different methods:

- The Clauser plot method with the van Driest logarithmic law. The van Driest logarithmic law provides a convenient way to estimate the flat-plate skin friction.
- The Clauser plot method with the Fenter-Stalmach logarithmic law.[10]

- The Preston tube method with the Bradshaw-Unsworth calibration equation.[12]
- The Preston tube method with the Allen calibration equation.[11]

The Clauser plot methods use rake data, and the Preston tube methods use Preston tube data.

The Clauser plot method fits the measured turbulent boundary-layer velocity profile to a compressible logarithmic law to get the skin friction value. Two different logarithmic laws were used, the van Driest and the Fenter-Stalmach logarithmic laws.

The Preston tube method (as outlined in reference 11) was used with the Bradshaw-Unsworth and the Allen calibration equations. These methods have been found[11] to provide the best correlations for compressible turbulent boundary layers.

Four different values of skin friction were computed from the wind-tunnel data using the appropriate theories. These values then were transformed into the incompressible plane using the van Driest II correlation and compared with the incompressible Karman-Schoenherr correlation as described in reference 9.

Figure 20 shows a plot of the results. The Reynolds number and the skin friction coefficient have been transformed into the incompressible plane to facilitate comparison with the Karman-Schoenherr correlation. The transformed Reynolds number based on momentum thickness is approximately 7.5×10^4 for Mach 2.0 flow, then increases to a maximum of 1.5×10^5 for Mach 0.7 flow before decreasing to approximately 8×10^4 for Mach 0.3 flow.

The majority of the results can be seen to agree with the Karman-Schoenherr correlation to approximately ±5 percent, which is within the expected accuracy of current skin friction theories and the uncertainties of the past data used to correlate these theories.[9] In general, the Clauser plot method used with the Fenter-Stalmach logarithmic law and the Preston tube method used with the Bradshaw-Unsworth equation correlate better with each other and with the Karman-Schoenherr theory than other methods do.

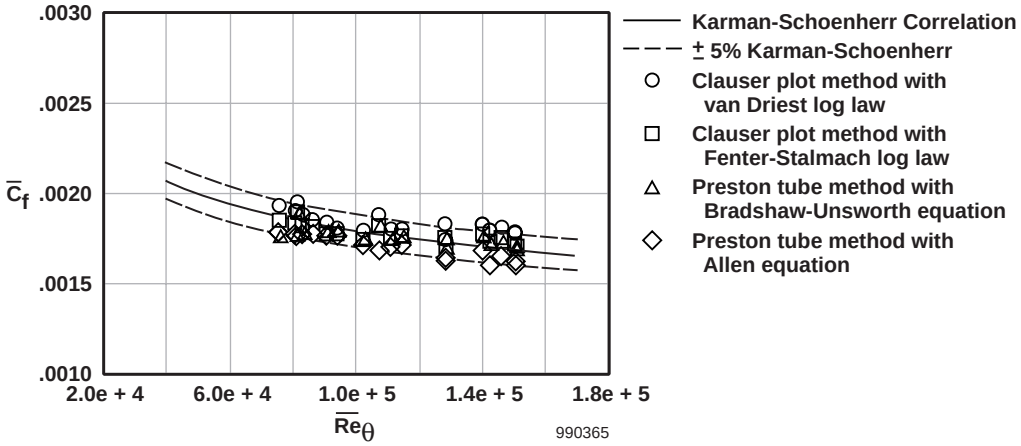

Figure 20. Skin friction coefficient distribution.

Conclusion

The design, fabrication, and wind-tunnel testing of a new, curved, boundary-layer rake have been described. This new boundary-layer rake will be used in F-15B/Flight Test Fixture flight research projects that require detailed surveys of the turbulent boundary layer. A design feature unique to this rake is its curved rake body, which allows pitot tubes to be clustered more densely in the near-wall region than conventional rakes allow.

The new rake was found to have good aerodynamic performance. The wind-tunnel test of the rake was conducted in the NASA Glenn Research Center 8×6 Supersonic Wind Tunnel at Mach numbers ranging from 0 to 2. The pitot pressures from the new rake agreed with data from a conventional rake over the range of Mach numbers tested. The boundary-layer profiles computed from the rake data were shown to have the standard logarithmic-law profile. Skin friction values computed from the rake data using the Clauser plot methods agreed with the Preston tube results and the van Driest II compressible skin friction correlation to approximately ±5 percent.

In addition to having good aerodynamic performance, the new rake design was found to be structurally rugged. Results from finite-element stress analysis of the new rake design showed very high factors of safety for both wind-tunnel and flight conditions. The rake also passed a ground vibration test in which random vibration measuring 12 *g* rms was applied for 20 min in each of the three normal directions.

References

[1]Richwine, David M., *F-15B/Flight Test Fixture II: A Test Bed for Flight Research*, NASA TM-4782, 1996.

[2]Clauser, Francis H., "Turbulent Boundary Layers in Adverse Pressure Gradients," *Journal of the Aeronautical Sciences*, Feb. 1954, pp. 91–108.

[3]Preston, J. H., "The Determination of Turbulent Skin Friction by Means of Pitot Tubes," *Journal of the Royal Aeronautical Society*, vol. 58, no. 518, Feb. 1954, pp. 109–121.

[4]Gracey, William, *Measurement of Aircraft Speed and Altitude*, NASA RP-1046, 1980.

[5]Grosser, Wendy I., *Factors Influencing Pitot Probe Centerline Displacement in a Turbulent Supersonic Boundary Layer*, NASA TM-107341, 1996.

[6]Gettelman, Clarence C., and Lloyd N. Krause, "Considerations Entering into the Selection of Probes for Pressure Measurement in Jet Engines," *Proceedings of the Instrument Society of America*, vol. 7, 1952, pp. 134–137.

[7]Allen, Jerry M., "Critical Preston-Tube Sizes," *Journal of Aircraft*, vol. 7, no. 3, May–June 1970, pp. 285-287.

[8]White, Frank M., *Viscous Fluid Flow*, 2nd ed., McGraw-Hill, Inc., Boston, Massachusetts, 1991.

[9]Hopkins, Edward J., and Mamoru Inouye, "An Evaluation of Theories for Predicting Turbulent Skin Friction and Heat Transfer on Flat Plates at Supersonic and Hypersonic Mach Numbers," *AIAA Journa*l, vol. 9, no. 6, June 1971, pp. 993–1003.

[10]Allen, Jerry M. and Dorothy H. Tudor, *Charts for Interpolation of Local Skin Friction From Experimental Turbulent Velocity Profiles*, NASA SP-3048, 1969.

[11]Allen, Jerry M., *Reevaluation of Compressible-Flow Preston Tube Calibrations*, NASA TM X-3488, 1977.

[12]Bradshaw, P. and K. Unsworth, "Comment on Evaluation of Preston Tube Calibration Equations in Supersonic Flow," *AIAA Journal*, vol. 12, no. 9, Sep. 1974, pp. 1293–1295.

REPORT DOCUMENTATION PAGE

Form Approved
OMB No. 0704-0188

1. AGENCY USE ONLY (Leave blank)	2. REPORT DATE	3. REPORT TYPE AND DATES COVERED
	January 2000	Technical Memorandum

4. TITLE AND SUBTITLE

Design and Evaluation of a New Boundary-Layer Rake for Flight Testing

5. FUNDING NUMBERS

WU 529-50-04-T2-RR-00-000

6. AUTHOR(S)

Trong T. Bui, David L. Oates, and Jose C. Gonsalez

7. PERFORMING ORGANIZATION NAME(S) AND ADDRESS(ES)

NASA Dryden Flight Research Center
P.O. Box 273
Edwards, California 93523-0273

8. PERFORMING ORGANIZATION REPORT NUMBER

H-2392

9. SPONSORING/MONITORING AGENCY NAME(S) AND ADDRESS(ES)

National Aeronautics and Space Administration
Washington, DC 20546-0001

10. SPONSORING/MONITORING AGENCY REPORT NUMBER

NASA/TM-2000-209014

11. SUPPLEMENTARY NOTES

Presented at 38th AIAA Aerospace Sciences Conference, Reno, Nevada, January 10–13, 2000, AIAA-2000-0503. Trong T. Bui and David L. Oates of NASA Dryden Flight Research Center; Jose C. Gonsalez, Dynacs Engineering Co., Inc., Brookpark, Ohio.

12a. DISTRIBUTION/AVAILABILITY STATEMENT

Unclassified—Unlimited
Subject Category 02, 34
Availability: NASA CASI (301) 621-0390
This report is available at http://www.dfrc.nasa.gov/DTRS/

12b. DISTRIBUTION CODE

13. ABSTRACT (Maximum 200 words)

A new boundary-layer rake has been designed and built for flight testing on the NASA Dryden Flight Research Center F-15B/Flight Test Fixture. A feature unique to this rake is its curved body, which allows pitot tubes to be more densely clustered in the near-wall region than conventional rakes allow. This curved rake design has a complex three-dimensional shape that requires innovative solid-modeling and machining techniques. Finite-element stress analysis of the new design shows high factors of safety. The rake has passed a ground test in which random vibration measuring 12 *g* rms was applied for 20 min in each of the three normal directions. Aerodynamic evaluation of the rake has been conducted in the NASA Glenn Research Center 8×6 Supersonic Wind Tunnel at Mach 0–2. The pitot pressures from the new rake agree with conventional rake data over the range of Mach numbers tested. The boundary-layer profiles computed from the rake data have been shown to have the standard logarithmic-law profile. Skin friction values computed from the rake data using the Clauser plot method agree with the Preston tube results and the van Driest II compressible skin friction correlation to approximately ±5 percent.

14. SUBJECT TERMS

Boundary layer, Compressible flows, Flight testing, Pitot pressure rake, Skin friction

15. NUMBER OF PAGES

22

16. PRICE CODE

A03

17. SECURITY CLASSIFICATION OF REPORT	18. SECURITY CLASSIFICATION OF THIS PAGE	19. SECURITY CLASSIFICATION OF ABSTRACT	20. LIMITATION OF ABSTRACT
Unclassified	Unclassified	Unclassified	Unlimited